Matti Karjalainen and Jyri Pakarinen, 2006, Wave digital simulation of a vacuum-tube amplifier, In: Proceedings of the 31st IEEE International Conference on Acoustics, Speech, and Signal Processing (ICASSP 2006), Toulouse, France, 14-19 May 2006, volume 5.

WAVE DIGITAL SIMULATION OF A VACUUM-TUBE AMPLIFIER

Matti Karjalainen and Jyri Pakarinen

Helsinki University of Technology
Laboratory of Acoustics and Audio Signal Processing
P.O.Box 3000, FI-02015 HUT, Finland

ABSTRACT

Virtual analog modeling is needed when simulating classic analog circuitry by DSP, for example when emulating analog sound synthesis and sound reproduction systems. In this paper we show how wave digital filters (WDFs) can be applied to efficient real-time simulation of vacuum-tube amplifier stages, typical in professional guitar amplifiers, which pose nonlinear behavior for desired distortion effects.

1. INTRODUCTION

Simulation of analog electronics by DSP is used nowadays extensively in music and audio technology. The goal is to approach the desirable sound of analog equipment, such as music synthesizers and reproduction systems, yet with the advantages of digital computation. Such virtual analog modeling seems straightforward but is found demanding due to nonlinearities and parametric variation in the analog domain. For example, tube amplifiers are preferred by many professional electric guitar players due to perceptually favorable distortion, producing a rich and warm sound. Real-time modeling of analog amplifiers accurately using DSP (see e.g. [1]) is a surprisingly demanding task, which only recently has resulted in good sound.

Analog circuit design is different from the development of DSP algorithms. Particularly in passive circuits the components interact in a bidirectional way with the neighboring components through the interconnection topology. The transfer properties of such circuitries can be approximated by DSP algorithms, for example by time-varying digital filters and memoryless nonlinearities. It would be desirable, however, to design a DSP-based simulator in a similar way as the analog circuitry, by connecting component blocks via terminals and ports.

Such an approach is in fact used in circuit simulators, such as SPICE [2, 3, 4]. Here we are interested, however, in efficient real-time simulation for music and audio applications. Wave digital filters (WDFs) are an example of a technique, which can be successfully applied to transforming analog circuits and networks into DSP-based equivalents [5, 6, 7]. In addition to the natural correspondence of the analog and digital formulations, WDFs have been found numerically robust and they can also support nonlinearities and time-varying components [9].

In this paper we study the applicability of WDFs to efficient real-time simulation of tube amplifier stages, typical in professional guitar amplifiers, generating nonlinear behavior for distortion effects. As a case study we take a triode tube amplifier, as shown by a schematic diagram in Fig. 1. In Section 2 the circuit is described briefly and the modeling of triode tube characteristics is presented. In Section 3 we introduce fundamentals of wave digital filters, particularly for implementing nonlinear elements, and derive different ways for realizing triode tube stages as WDF circuits. The results

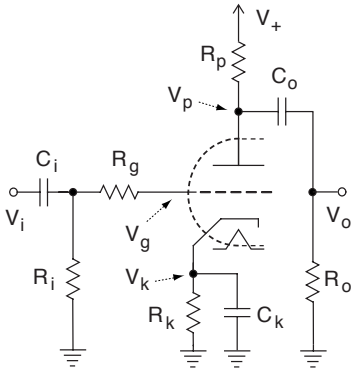

Fig. 1. A typical triode amplifier stage.

are analyzed in Section 4 for the amplifier stage of Fig. 1, including computational efficiency of implementations on a WDF-based modeling platform. Finally we discuss the possibilities to generalize the approach to more generic modeling cases, including electro-mechanical-acoustical systems.

2. TRIODE TUBE AND AMPLIFIER STAGE

Figure 1 depicts the schematic diagram of a typical triode stage used in audio amplifiers. Input signal V_i is passed through DC voltage separation high-pass of C_i and R_i. Then it is fed to the grid of the triode tube. The resistor R_g may be used to limit grid current for positive grid-to-cathode voltages $V_\mathrm{gk} = V_\mathrm{g} - V_\mathrm{k}$ as well as to avoid instabilities. The cathode resistor R_k is used to make a desired negative bias for V_gk, and the capacitor C_k makes a by-pass for R_k at audio frequencies.

The plate circuit of the triode consists of the plate resistor R_p feeding the supply voltage V_+. The plate voltage V_p is taken to output V_o through C_o and R_o to separate the DC component of V_p.

The plate current through the triode depends on V_gk as well as V_pk, the plate-to-cathode voltage. The tube works as a nonlinear voltage-controlled resistor. For an idealized triode[1] the plate current I_p depends on the plate-to-cathode voltage V_pk and grid-to-cathode voltage V_gk according to [10]:

$$I_\mathrm{p} = f(V_\mathrm{gk}, V_\mathrm{pk}) = K(\mu V_\mathrm{gk} + V_\mathrm{pk})^{3/2}, \qquad (1)$$

where μ is the voltage gain of the triode for constant plate current and K is another tube-specific constant. This model is not accurate enough for our purposes, however. It is possible to fit more accurate formulas to measured tube data, and we have adopted an experimentally well fitted model given in [11]:

[1] A similar formulation could be made also for a pentode tube.

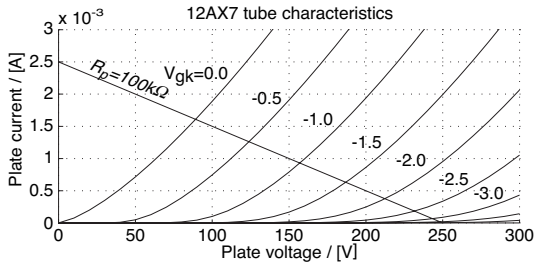

Fig. 2. Characteristics of triode 12AX7 according to Eqs. (2) and (3) and tube parameter values given in the text. V_{gk} is the grid-to-cathode voltage, and a load line for $R_{\mathrm{p}} = 100$ kΩ and $V_{+} = 250$ V is drawn.

$$I_{\mathrm{p}} = \frac{E_1^{k_{\mathrm{x}}}}{k_{\mathrm{g1}}}(1 + \mathrm{sign}(E_1)), \qquad \text{where} \tag{2}$$

$$E_1 = \frac{V_{\mathrm{pk}}}{k_{\mathrm{p}}} \log(1 + \exp(k_{\mathrm{p}}(\tfrac{1}{\mu} + V_{\mathrm{gk}}/\sqrt{k_{\mathrm{vb}} + V_{\mathrm{pk}}^2}))) \tag{3}$$

and μ is as in Eq. (1), and k_{x}, k_{g1}, k_{p}, and k_{vb} are other tube-specific constants. For the triode 12AX7, a typical preamplifier tube, the parameter values are [11]:

μ	k_{x}	k_{g1}	k_{p}	k_{vb}
100	1.4	1060	600	300

Figure 2 plots the characteristics of triode 12AX7 as well as a plate resistor load line for $R_{\mathrm{p}} = 100$ kΩ and $V_{+} = 250$ V.

3. WDF MODELING OF NONLINEAR CIRCUITS

In this section we first present basics of wave digital filters, including nonlinearities, and then derive different realizations of the tube model.

3.1. Basics of WDFs

Wave digital filters are certain types of digital filters with valid interpretations in the physical world. This means that they can simulate the behavior of a physical system so that the filter coefficients depend on the parameters of this physical system. WDFs are modular, which makes them especially well-suited for modeling block-based networks, such as electric circuits. More information about the properties of WDFs can be found, e.g., in [6, 8, 5].

WDF elements are connected to each other using ports, see Fig. 3(a). For each port, a port voltage V and a port current I can be defined. However, instead of using this Kirchhoff pair, WDF elements operate using wave variables a and b

$$\begin{bmatrix} a \\ b \end{bmatrix} = \begin{bmatrix} 1 & R_0 \\ 1 & -R_0 \end{bmatrix} \begin{bmatrix} V \\ I \end{bmatrix}, \tag{4}$$

where a denotes the wave component coming to the element, and b denotes the wave component leaving the element. R_0 is a port resistance parameter, which relates the Kirchhoff variables via Ohm's law. It must be noted that R_0 can have any nonnegative value, so that it can be used as an additional degree of freedom for simplifying calculations.

Basic one-port WDF components, shown in Fig. 3(b)-(e), correspond to the basic electric circuit elements, namely resistors, capacitors, inductors, and voltage sources. The multi-port elements shown in Fig. 3(f) and 3(g) denote the series and parallel adaptors, respectively. These adaptors implement the wave scattering in series and parallel connections, and enable connecting one-port elements together. When interconnecting WDF elements, computational problems may arise due to delay-free loops. This can be avoided by properly selecting the port resistances so that certain signal paths become disconnected. For example, if the series adaptor's (Fig. 3(f)) third port is set to have a resistance value of

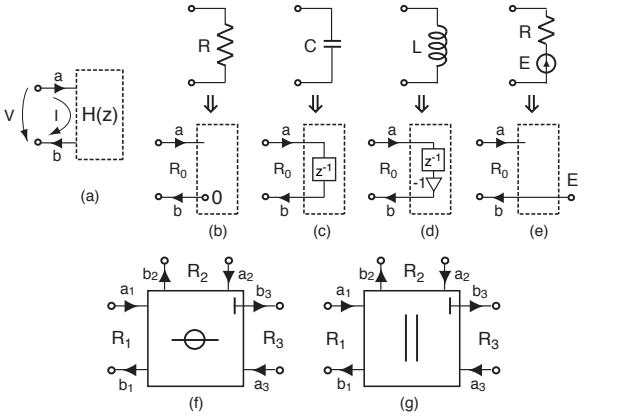

Fig. 3. Basic WDF components used for constructing circuits: (a) general one-port, (b) resistor: $R_0 = R$, (c) capacitor: $R_0 = T/2C$, (d) inductor: $R_0 = 2L/T$, (e) voltage source: $R_0 = R$, (f) series adaptor, and (g) parallel adaptor, where T is sample period.

$$R_3 = R_1 + R_2, \tag{5}$$

the outgoing wave b_3 becomes independent of the incoming wave a_3, and the third port is called an adapted (or reflection-free) port. Similarly, for the parallel adaptor (Fig. 3(g)), if we set

$$R_3 = R_1 R_2/(R_1 + R_2), \tag{6}$$

the third port becomes adapted. The adapted ports are denoted by drawing a '$\vdash$'-shaped ending for the outgoing terminal, as shown in Figs. 3(f) and 3(g). Clearly, both serial and parallel adaptors can only have a single adapted port.

When connecting several WDF elements together, the modeling network can be represented as a binary connection tree (BCT), where every one-port element is connected to a three-port adaptor and the adapted port of this adaptor further to the next adaptor [13]. The adaptor elements are called nodes, and the one-port elements are called the leaves of the BCT. The network operates by calculating the outgoing wave variables and port resistance values starting from the leaves and gradually proceeds towards a predefined root node. This root node calculates its outgoing wave using the incoming waves and the port resistance information. After this, the wave leaving the root node is distributed as an incoming wave for the leaves via the nodes.

Note that the propagation of waves from the leaves to the root node is possible even though the waves traveling to the other direction are not evaluated yet. This is because adapted ports are used so that the waves traveling toward the root become independent of the waves traveling away from the root.

3.2. WDF nonlinearities

Modeling of a one-port nonlinearity with WDFs means that the a-to-b reflection function of the element is nonlinear and the port resistance varies as a function of the incoming wave. Generally, the nonlinearity can be reactive (i.e., has memory), but since the main interest here is tube amplifier modeling, we consider only resistive (memoryless) nonlinearities. More information on nonlinear WDFs can be found for example in [9, 12].

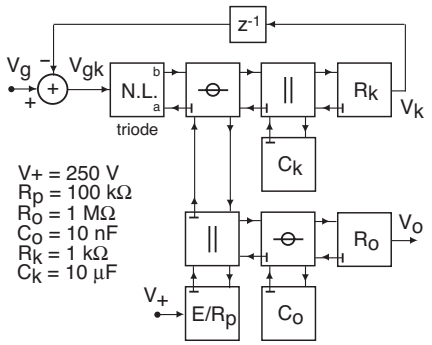

Fig. 4. WDF binary tree for simulation of the triode stage in Fig. 1. The input circuit (C_i, R_i, R_g) is omitted and the cathode voltage V_k is used throught a unit delay to get the grid-to-cathode voltage V_gk.

A nonlinear resistor can be implemented directly using the function of nonlinear characteristics $I = f(V)$. This will be discussed in Section 3.4. The a-to-b relation is solved iteratively. However, it is more efficient to implement the complicated nonlinearity as a lookup-table, and it is required when the nonlinear function is unknown. For vacuum-tubes, data sheets describing the V-I characteristics can be found on the Internet, e.g., [14]. Details about using nonlinear lookup-tables will be discussed in Section 3.5.

It is advisable to connect the nonlinear element at the adapted port of the root node when using a BCT network. If it were connected as a leaf, the wave going into the nonlinear element would change its port resistance, and this change would have to be propagated to all other port resistances of the path towards the root, thus requiring iterative re-evaluation of the whole system. As a consequence, if efficient WDF modeling is desired, the BCT can only support one nonlinear element. More nonlinearities can be added to the simulation in a similar way as far as they are connected through delay elements.

3.3. WDF modeling of the triode stage

The triode amplifier stage in Fig. 1 can be simulated by the WDF approach easily except the tube itself, which acts as a voltage-controlled nonlinear resistor. When building a WDF tube element, the task is to implement the given tube characteristics $I_\mathrm{p} = f(V_\mathrm{gk}, V_\mathrm{pk})$ as defined by Eqs. (3)-(2). Using also Eq. (4) we get an implicit pair of equations

$$V_\mathrm{pk} + R_0 f(V_\mathrm{gk}, V_\mathrm{pk}) - a = 0 \tag{7}$$

$$b = V_\mathrm{pk} - R_0 f(V_\mathrm{gk}, V_\mathrm{pk}), \tag{8}$$

where V_gk and the port resistance R_0 of the tube's plate-cathode series connection are known. Figure 4 shows a binary tree WDF structure for the tube (N.L.) and the plate-cathode circuit of Fig. 1. To simplify the task, we have assumed that the grid circuit can be computed independently of the plate-cathode circuit. We also assume that the cathode voltage is changing slowly compared to audio signals, so that the grid-to-cathode voltage V_gk can be obtained from the previous value of the cathode voltage V_k, i.e.,

$$V_\mathrm{gk}(n+1) = V_\mathrm{g}(n+1) - V_\mathrm{k}(n). \tag{9}$$

3.4. Tube modeling by iteration

If the grid voltage V_gk is known, the tube behavior can be approximated by numerically solving Eq. (7) with respect to the plate voltage V_pk in a recursive loop. Note that the incoming wave variable a is obtained by propagating the waves from the leaves to the root node. While there are many iteration techniques to choose from, see e.g. [15], we used the Newton-Raphson method. In the case of the WDF tube, this algorithm can be stated as

$$V_\mathrm{pk}(n+1) = V_\mathrm{pk}(n) - \frac{f(V_\mathrm{pk}(n))}{f'(V_\mathrm{pk}(n))}, \tag{10}$$

where n denotes the index of the iteration step, $f(V_\mathrm{pk}(n))$ is the left-hand side expression in Eq. (7), and $f'(V_\mathrm{pk}(n))$ is its derivative. The first value of the plate voltage can be initially chosen anywhere within the operating range, i.e., $V_\mathrm{pk}(0) \in [0, 250]$, and for the next sample steps the previous value can be used for iteration. Finally, the reflected wave b is obtained from Eq. (8).

Although the Newton-Raphson algorithm converges relatively fast when numerically evaluating Eq. (7), optional iteration techniques, such as the golden section method or the Fibonacci search, could be used instead. The convenience of these algorithms is that they do not require the derivative of the nonlinear function to be approximated. This reduces the number of nonlinear function evaluations per iteration step to unity, and can be advantageous if the evaluation takes a lot of time. On the other hand, these techniques generally require more iteration steps for achieving the same accuracy as the Newton-Raphson algorithm. Iteration techniques might provide useful even if the nonlinear V-I relation of the tube is stored in a pre-calculated lookup table.

3.5. Tube modeling by table lookup

If the tube characteristics can be fixed at compile time, it is possible to precompile a lookup table and use interpolation to efficiently compute the wave scattering due to the triode nonlinearity.

The most efficient way is to compile a two-dimensional lookup-table for wave variable reflection function $b = g(a, V_\mathrm{gk})$. This means solving of the implicit Eqs. (7)-(8) numerically at compile time for (a, b) pairs (R_0 must be fixed), so that a is discretized by a uniform step size, and for a set of grid-to-cathode voltages V_gk uniformly in the operating range of the triode. Then at runtime there is only a need to look for the b-values for two nearest indices of given a and two nearest indices for V_gk in the table. Linear 2-D interpolation between these four b-values yields the b that is reflected back from the triode block to the wave port of the root node, see Fig. 4.

3.6. Tube modeling by table lookup and iteration

The most straightforward way from the point of view of the compilation phase is to store the lookup table in (V, I) pairs. In this case, iterative search is needed as in subsection 3.4, but now the mapping $I_\mathrm{p} = f(V_\mathrm{gk}, V_\mathrm{pk})$ is still obtained quickly from a 2-D lookup table. Such iteration is naturally slower than the direct a-b mapping.

4. PERFORMANCE ANALYSIS

There are two further problems that usually require oversampling in order to get good simulation results in nonlinear WDF circuits. The first one is that WDF realizations of capacitors and inductors are made through bilinear mapping, which causes frequency warping of related high-frequency responses [5]. The second problem is the potential of aliasing with nonlinear operations. To avoid harmonic and intermodulation products to fold back to the Nyquist baseband, oversampling factors of 2-8 may be needed. On the other hand, oversampling reduces the required steps in iterative algorithms.

The three implementation methods described in Section 3 for the WDF structure of Fig. 4 were simulated using the BlockCompiler real-time modeling environment [16] on a 1.67 GHz PowerPC

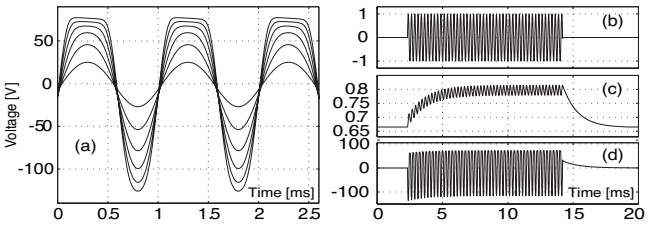

Fig. 5. (a) Distortion in the triode stage: output signal for 1 kHz sine wave input of amplitudes from 0.25 to 1.5 in steps of 0.25 Volts. (b) Sine burst grid input, (c) cathode voltage, and (d) output voltage.

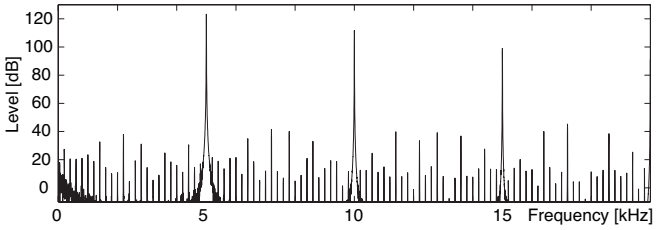

Fig. 6. Spectrum (0-20 kHz) of distorted 5 kHz sine wave (1.25 Volts input), including the aliased components, for four times oversampling.

processor (Macintosh Powerbook G4). The following table presents the computational loads for the sample rate of 44100 Hz.

Method	μs/cycle	% CPU
Iteration of equations, 1 iteration/sample	1.17	5.16
Table-based iteration, 1 iteration/sample	0.31	1.37
Direct a-b table lookup	0.18	0.79

It can be concluded that iteration of the original equations is expensive if oversampling or multiple step iteration is used. Table-based iteration is much faster. The direct a-b table lookup is naturally the fastest, being useful in practical audio effects design.

The smoothly increasing distortion behavior of the tube stage can be seen in Fig. 5(a), where the amplifier is driven by a 1 kHz sine wave for successively increasing input amplitudes.

A characteristic feature of the tube amplifier is that for signals of varying amplitudes the bias (operating point) of the tube varies with the time constants of the RC-circuits, which may add to the richness of sound. This effect is seen in Fig. 5(b)-(d) where the grid, cathode, and output voltages are plotted for a sine burst input.

Aliasing at high driving levels can be perceptually severe without oversampling. Figure 6 shows a case where the oversampling factor of four has been applied to strong distorting of a 5 kHz sinusoid. The aliased components are 70-80 dB below the signal peaks up to 10 kHz. In practice this aliasing cannot be perceived in playing the electric guitar at such a distortion level.

5. DISCUSSION

In this paper we have formulated a WDF approach to the modeling of tube amplifier stages that exhibit intentional distortion, e.g., in guitar amplifiers. It is to be noticed that the WDF-based approach may not be the computationally most efficient one, when compared to straightforward digital filtering and nonlinearities, for example. The advantage of the WDF formulation is the systematic mapping from an analog circuit to a digital block-wise realization. This is useful in rapid prototyping of analog amplifiers as well as in virtual analog synthesis of classical tube amplifiers.

The WDF modeling of a multi-stage amplifier is straightforward as far as the stages between tubes in a full-scale amplifier can be computed independently. In general this is not possible. Already the capacitive feedback from plate to grid needs to be modeled to obtain correct high-frequency behavior. Any feedback in the system makes the modeling harder, since delays in loops shorter than the unit delay require iterative solutions or oversampling, i.e., more complicated and computationally more expensive algorithms.

Many other questions arise when generalizing the WDF approach. For example the effect of the grid current for positive grid-cathode voltages was omitted above. In fact, the tube should be modeled as a nonlinear multi-port.

In spite of these challenging questions, the WDF approach shows potential as a systematic way to simulate nonlinear analog amplifiers and sound reproduction systems in real time.

6. ACKNOWLEDGMENTS

Jyri Pakarinen's research has been funded by the Academy of Finland (project 104934), S3TK graduate school, Tekniikan edistämissäätiö, and Nokia Foundation. We acknowledge fruitful discussions with Cumhur Erkut and Antti Huovilainen.

7. REFERENCES

[1] M. Karjalainen, T. Mäki-Patola, A. Kanerva, A. Huovilainen, and P. Jänis, "Virtual Air Guitar," *Proc. 117th AES Convention*, preprint 6203, San Francisco, CA, USA, 2004.

[2] http://bwrc.eecs.berkeley.edu/Classes/IcBook/SPICE/

[3] www.orcad.com/community.aspx

[4] W. M. Leach, Jr., "SPICE Models of Vacuum-Tube Amplifiers," *J. Audio Eng. Soc.*, Vol. 43, No. 3, 1995, pp. 117-126.

[5] A. Fettweis, "Wave Digital Filters: Theory and Practice," *Proc. of the IEEE*, Vol. 74, No. 2, pp. 270-327, 1986.

[6] J. O. Smith, *Physical Audio Signal Processing*, August 2004 Draft http://ccrma.stanford.edu/∼jos/pasp/.

[7] V. Välimäki, J. Pakarinen, C. Erkut, and M. Karjalainen, "Discrete-time Modelling of Musical Instruments", *Reports on Progress in Physics*, Vol. 69, No. 1, pp. 1-78, Jan. 2006.

[8] S. Bilbao, "Wave and Scattering Methods for Numerical Simulation," Wiley, 2004.

[9] A. Sarti and G. De Poli, "Toward nonlinear wave digital filters," *IEEE Trans. Signal Proc.*, Vol. 47, No. 6, pp. 1654-1668, 1999.

[10] K. R. Spangenberg, *Fundamentals of Electron Devices*, McGraw-Hill, New York, 1957.

[11] www.normankoren.com/Audio/Tubemodspice_article.html

[12] F. Pedersini, A. Sarti, and S. Tubaro, "Object-based sound synthesis for virtual environment using musical acoustics," *IEEE Signal Proc. Magazine*. Vol. 17, No. 6, pp. 3751, 2000.

[13] G. De Sanctis, A. Sarti, and S. Tubaro, "Automatic synthesis strategies for object-based dynamical physical models in musical acoustics," *Proc. Int. Conf. in Digital Audio Effects (DAFx-03)*, London, UK, September 8-11, 2003.

[14] http://www.duncanamps.com/

[15] M. S. Bazaraa, H. D. Sherali and C. M. Shetty, *Nonlinear Programming Theory and Algorithms*, 2nd ed., Wiley, 1993.

[16] M. Karjalainen, "BlockCompiler: Efficient Simulation of Acoustic and Audio Systems," *Proc. 114th AES Convention*, preprint 5756, Amsterdam, Netherlands, 2003.